


# Knockdown of Annexin-A1 Inhibits Growth, Migration and Invasion of Glioma Cells by Suppressing the PI3K/Akt Signaling Pathway

ASN Neuro  
Volume 13: 1–16  
© The Author(s) 2021  
Article reuse guidelines:  
sagepub.com/journals-permissions  
DOI: 10.1177/17590914211001218  
journals.sagepub.com/home/asn



Liqing Wei<sup>1,\*</sup>, Li Li<sup>2,\*</sup>, Li Liu<sup>3,\*</sup>, Ru Yu<sup>3,\*</sup>, Xing Li<sup>4</sup>, and Zhenzhao Luo<sup>1</sup> 

## Abstract

ANXA1, which can bind phospholipid in a calcium dependent manner, is reported to play a pivotal role in tumor progression. However, the role and mechanism of ANXA1 involved in the occurrence and development of malignant glioma are still not well studied. Therefore, we explored the effects of ANXA1 on normal astrocytes and glioma cell proliferation, apoptosis, migration and invasion and the underlying mechanisms. We found that ANXA1 was markedly up-regulated in glioma cell lines and glioma tissues. Down-regulation of ANXA1 inhibited normal astrocytes and glioma cell proliferation and induced the cell apoptosis, which suggested that the consequences of loss of Annexin I are not specific to the tumor cells. Furthermore, the siRNA-ANXA1 treatment significantly reduced tumor growth rate and tumor weight. Moreover, decreasing ANXA1 expression caused G2/M phase arrest by repressing expression levels of cdc25C, cdc2 and cyclin B1. Interestingly, ANXA1 did not affect the expressions of  $\beta$ -catenin, GSK-3 $\beta$  and NF- $\kappa$ B, the key signaling molecules associated with cancer progression. However, siRNA-ANXA1 was found to negatively regulate phosphorylation of AKT and the expression and activity of MMP2/-9. Finally, the decrease of cell proliferation and invasiveness induced by ANXA1 down-regulation was partially reversed by combined treatment with AKT agonist insulin-like growth factor-I (IGF-I). Meanwhile, the inhibition of glioma cell proliferation and invasiveness induced by ANXA1 down-regulation was further enhanced by combined treatment with AKT inhibitor LY294002. In summary, these findings demonstrate that ANXA1 regulates proliferation, migration and invasion of glioma cells via PI3K/AKT signaling pathway.

## Keywords

RNA interference, ANXA1, U87 cells, cell growth, migration and invasion

Received February 15, 2021; Revised February 15, 2021; Accepted for publication February 18, 2021

## Introduction

Gliomas are common intracranial primary tumors in both children and adults, which are prone to metastasis, and have poor prognosis. The median survival time of glioblastoma is only about one year (Fatehi et al., 2018; Góralaska et al., 2018). Although the treatments of glioma including diagnostic modalities, and surgery combined with chemotherapy, radiotherapy and biological therapy, have been continuously improved in recent years, the therapeutic effect is still not satisfactory (Nishikawa, 2010; Lei et al., 2015). In-depth study of the molecular mechanisms of glioma, and effective strategies for glioma are urgently needed.

The phosphoinositide-3-kinase/protein kinase B (PI3K/Akt) signaling pathway plays a key role in

<sup>1</sup>Department of Medical Laboratory, The Central Hospital of Wuhan, Tongji Medical College, Huazhong University of Science and Technology, Wuhan, China

<sup>2</sup>Department of Pathology, The Central Hospital of Wuhan, Tongji Medical College, Huazhong University of Science and Technology, Wuhan, China

<sup>3</sup>Department of Respiration, The Children's Hospital of Wuhan, Tongji Medical College, Huazhong University of Science and Technology, Wuhan, China

<sup>4</sup>Department of Neurobiology, The School of Basic Medical Science, Tongji Medical College, Huazhong University of Science and Technology, Wuhan, China

\*These authors contributed equally to this work.

### Corresponding Author:

Zhenzhao Luo, Department of Medical Laboratory, Central Hospital of Wuhan, 26 Shengli St., Jiangnan District, Wuhan 430014, China.  
Email: lzzbvy@163.com



regulating cell cycle, apoptosis, motility, adhesion, and cancer progression (Laplante and Sabatini, 2009). It was shown that PI3K/Akt signaling pathway was inappropriately activated frequently in human glioma cells (Akhavan et al., 2010; Zhong et al., 2019). The PI3K/Akt signaling pathway plays a vital role for the proliferation and invasiveness of glioma cells. PI3Ks are heterodimers, comprising of one catalytic subunit p110 encoded by the genes PIK3CA (p110 $\alpha$ ), PIK3CB (p110 $\beta$ ) or PIK3CD (p110 $\delta$ ), whereas one regulatory subunit p85 encoded by PIK3R1 (p85 $\alpha$ ), PIK3R2 (p85 $\beta$ ) or PIK3R3 genes (p85 $\gamma$ ) (X. Wang et al., 2015). Akt is a serine-threonine kinase which serves as a downstream effectors of PI3K, promoting cancer cells survival, proliferation and angiogenesis (Danielsen et al., 2015). It has been reported that the PI3K/Akt signaling pathway is dysregulated in one-third of human cancers (Faes and Dormond, 2015; Guerrero-Zotano et al., 2016). Pioneer studies demonstrated that high expression of p-Akt was associated with poor survival, progressive high-grade, as well as intracranial invasion in glioma patients (Chai et al., 2018; Sun et al., 2018), indicating that modulation of the PI3K/Akt signal transduction is a promising therapeutic strategy in gliomas.

Annexin-A1 (ANXA1)-mediated signaling has received increasing attentions in the development of human tumors (Foo et al., 2019). Recent investigations prove that ANXA1 plays a pivotal role in membrane aggregation, proliferation, apoptosis, phagocytosis and carcinogenesis (Lim and Pervaiz, 2007). ANXA1 is highly expressed in hepatocellular carcinoma (Masaki et al., 1996), adenocarcinomas of the esophagus (Kan and Meltzer, 2009) and pancreatic cancer (Bai et al., 2004), lung adenocarcinoma (Liu et al., 2011) and glioma (Cheng et al., 2013), down-regulation or deletion in adenocarcinoma of prostate (Patton et al., 2005), cervical cancer (L. D. Wang et al., 2008), thyroid cancer (Petrella et al., 2006), head and neck cancer (Garcia Pedrero et al., 2004). Although the overexpression of ANXA1 in glioma has been reported, its role and underlying mechanisms in regulating the proliferation, migration and invasion of glioma have not been fully elucidated.

The disintegration of the tumor matrix and the secretion of MMPs from tumor cells facilitate the migration and invasion of glioma cells. Previous studies have correlated the expression of proteolytic enzymes such as matrix metalloproteinases (MMP)-2/-9 and vascular endothelial growth factor (VEGF) with migration and invasion of human GBM cells, indicating the significance of these proteins in the occurrence and development of cancers (Pagliara et al., 2014). Bizzarro *et al.* showed that ANXA1 promoted invasion by FPR1 and FPR2, in prostate cancer cells, possibly through increasing activity and expression of MMP-2/-9 (Bizzarro et al., 2015). In the

melanoma cancer cells, ANXA1 induced invasiveness by promoting MMP-2 expression (Boudhraa et al., 2014). Gastardelo *et al.* demonstrated that stimulated of Hep-2 tumor cells with the ANXA1 mimetic peptide Ac2-26 down-regulated the expression of the MMP-2, while up-regulated that of the MMP-9 (Gastardelo et al., 2014).

Therefore, this study aims to further confirm the role and underlying mechanisms of ANXA1 in the cell growth, migration and invasion of glioma. Our results found that decreasing ANXA1 expression significantly inhibited the proliferation, migration and invasion of human glioma cells, which was partly attributed to the inhibition of PI3K/Akt signaling pathway and the down-regulation of the expression and activity of MMP-2/-9. Our results suggested that ANXA1 could be a potential therapeutic target for the treatment of glioma.

## Materials and Methods

### Cells and Reagents

Several human glioma cell lines (U87, U251, U118 and A172) and normal brain glial cell lines (HEB) were obtained from the Institute of Biochemistry and Cell Biology of Chinese Academy of Sciences (Shanghai, China), and the normal human astrocytes (NHA, Cat. #CC2565) was obtained from the Lonza Group Ltd (Basel, Switzerland). All the cells were cultured in DMEM medium (Gibco, Cat. #11965092, Carlsbad, CA, USA) supplemented with 10% of fetal bovine serum (FBS, Gibco, Cat. #16140089, USA) at 37°C with 5% CO<sub>2</sub> humidified atmosphere. Cells in logarithmic growth were used for experiments, the maximum number of passages for cell lines was <10. Additionally, 5  $\mu$ M LY294002 (#19-142, Sigma, St. Louis, MO, USA) was added into the Akt inhibitor group and 20  $\mu$ g/ml IGF (#291-G1-200, R&D Systems, Minneapolis, MN) was added to the Akt agonist group. The siRNA is an interference sequence with a significant interference effect in the literatures (Yang et al., 2011; Pin et al., 2012). The siRNA negative control is a negative control sequence that does not have any match with the human genome sequence (si-NC, GenePharma Co., Shanghai, China). The transfection reagent Lipofectamine RNAiMAX (#13778150), Opti-MEM media (#31985070) were purchased from Invitrogen (Carlsbad, CA, USA), Trizol, Moloney's murine leukemia reverse transcriptase (M-MLV) and Taq enzyme were purchased from Applied Biosystems (#4368813), and the primers were synthesized by Shanghai Invitrogen Co., Ltd. The sources of antibodies were as follows: p110  $\alpha$  (#4255), p85 (#4292), MMP-2 (#40994), MMP-9 (#3852),  $\beta$ -catenin (#9562), ANXA1 (#3299), p-Akt<sup>(Ser473)</sup> (#4060), Akt (#4685),  $\beta$ -actin (#3700),

cdc2 (#28439), Cyclin D1 (#2922) and horseradish peroxidase (HRP)-The second antibody (#7074 or #7076) were obtained from Cell Signaling Technology (Danvers, MA, USA). VEGF ELISA Kits (#QVE00B), Cdc25 (#MAB4459-SP) and cyclinB1 (#AF6000-SP) antibody were purchased from American R&D Company (R&D Systems, Minneapolis, MN). 1-Stearoyl-2-[1-<sup>14</sup>C] arachidonoyl-*sn*-glycero-3-phosphocholine (2-AA-PC; 56.0 mCi/mmol) was obtained from Amersham Pharmacia Biotech (Buckinghamshire, UK) and used as the substrate. Unlabeled 2-AA-PC and Scintillation fluid (Aquasol-2) were obtained from Sigma (St. Louis, MO, USA). The crystal violet dye (#DC079-1G) was obtained from Beijing Dingguo Biological Co., Ltd., and the transwell chambers (#3422) were purchased from Corning Lifesciences (Kennebunk, ME, USA), Matrigel (#356234) were obtained from BD Biosciences (Franklin Lakes, NJ, USA). The pore size of the transwell chamber membrane was 8  $\mu$ m.

### Tissue Specimens

58 cases of glioma paraffin archived surgical specimens from June 2013 to August 2019 in the Department of Neurosurgery, the Central Hospital of Wuhan, including 31 males and 27 females; aged 18-63 years. All cases were diagnosed by pathological examination, and 3 non-tumor brain tissues (NBT) obtained by decompression of craniocerebral injury were selected as controls. All patients have detailed clinical data. According to the 2000 WHO central nervous system tumor classification criteria, there were 15 cases of grade II, 16 cases of grade III, and 27 cases of grade IV. Meanwhile, 3 cases of grade IV and 3 cases of non-tumor brain tissues were collected and liquid nitrogen cryopreserved for Western blot analysis. This study protocol was approved by Ethics committee of The Central Hospital of Wuhan and a consent signed form was obtained from all participants.

### Western Blot Analysis

Total proteins were prepared from glioma cells, normal human astrocytes or brain tissues and equal amount of proteins were loaded for immunoblot analysis. The proteins were separated by 10% SDS-PAGE and subsequently transferred to a polyvinylidene fluoride (PVDF) membranes (#ISEQ00010, Millipore, Billerica, Massachusetts, USA), rinsed three times with Tris-buffered saline containing 0.1% Tween 20 (TBST), and then blocked with 5% of non-fat milk in TBST at room temperature for 1 h, then the membranes were subsequently incubated with corresponding primary antibodies of 1:1000 in TBST at 4°C overnight. After washing with

TBST thrice and the membranes were then subsequently incubated with the horseradish peroxidase-conjugated secondary antibodies of 1:10000 in TBST at room temperature for 1 h. After washing with TBST, the membranes were visualized by enhanced chemiluminescence kit (#RPN2232, Amersham, GE Health, UK) and photographed. ImageJ1.4.3 (National Institutes of Health, Bethesda, MD, USA) analyzed the gray values of each band with  $\beta$ -actin as a loading control.

### Transfection of U87 Cells With siRNA

U87 cells were passaged 24 h before transfection, inoculated into 35 mm culture dishes at a density of  $5 \times 10^5$  cells per well, and cell confluence reached 70% for transfection. The blank control group was untransfected, the negative control group was transfected with siRNA negative control sequence, and the siRNA interference group was transfected with ANXA1 interference sequence. One hour before cell transfection, 1.5 ml of serum-free medium opti-MEM was replaced. The negative control sequence, ANXA1 interference sequence and Lipofectamine 2000 were resuspended in 500  $\mu$ l serum-free medium opti-MEM, the final concentration of three siRNA interference chains and one siRNA negative control was 100 nmol/L, and the mixture was allowed to stand at room temperature for 20 min, and the complex was added to the cell culture, after incubating for 6 hours in the incubator, then the transfection medium was replaced with complete medium, and the subsequent culture was used for subsequent experiments from 24–72 h. The siRNA duplex sequences (Shanghai GenePharma Co.) selected for this study was listed as follows: siRNA1: 5'-ATGCCTCACAGCTATCGTGAA-3'; siRNA2: 5'-UGACCGAUCUGAGGACUUU-3'; siRNA3: 5'-CAAGGU GGUCCCGGAUCA-3'.

### Real-Time RT PCR

Total RNA was separately extracted from glioma cells 48 h after transfection, and reverse transcription PCR was performed. GAPDH was chosen as an internal control. The primer sequences used were shown as follows: ANXA1 forward, 5'-GGTGTGAATGAAGACTTGGCTGA-3', and the reverse, 5'-GTTTCATCCAGGATGGCTTGGA-3'; GAPDH forward, 5'-AAGGTGAAGGTCGGAGTCAAC-3', and the reverse, 5'-GGGGTCATTGATGGCAACAATA-3'. The reaction system was performed by using the Fast SYBR<sup>TM</sup> Green MasterMix Kit (Cat. #4385610, Life Technologies, Carlsbad, CA, USA) according to manufacturer's protocols. The reaction conditions were: pre-denaturing at 95°C for 30 sec, 95°C for 5 sec, 60°C for 26 sec for a total of 40 cycles. The relative ANXA1 mRNA expression was quantified by  $2^{-\Delta\Delta Ct}$  comparative method.

### Cell Counting Kit-8 (CCK-8) Assay and TUNEL Assay

U87 cells from each group were harvested 24 h after transfection and plated at a density of  $2 \times 10^3$  cells in a 96-well plate. Cells from each group were cultured for 24, 48, 72h and 96 h before CCK-8 assay kit (#CK-04, Dojindo, Kumamoto, Japan) was applied and 10  $\mu$ l reaction solution was added to each well and subsequently incubated for 10 min. The absorbance was then detected by an EnSpire Manager spectrophotometer plate reader (Turku, Singapore) at 450 nm (excitation) and 600 nm (emission). For the survival assays, cells that had undergone the indicated treatments were fixed in 4% formaldehyde for 20 min and permeabilized with 0.1% Triton X-100. Thereafter, the glioma cells were incubated with 50  $\mu$ l/well TUNEL reaction mixture for 1 h at 37°C. The cells were then examined and counted immediately under fluorescence microscopy (IX81, Olympus, Japan).

### Flow Cytometry Analysis

U87 cells in log-phase were seeded at a density of  $4 \times 10^5$  cells in 6-well plates. Cells were collected at 48 h after transfection. The analysis of cell cycles and apoptosis was performed by using flow cytometer (BD Biosciences, NJ, USA). For cell cycle examination, an EZCell™ Cell Cycle Analysis kit (#558622, BD Bioscience, San Jose, CA, USA) was utilized. For cell apoptotic rates determination, we used a Annexin V-FITC/PI cell apoptosis analysis kit (#556547, BD Bioscience, San Jose, CA, USA).

### Migration and Invasion Assay

First placed the Transwell chamber in a liquid containing DMEM + 0.1% BSA (bovine serum albumin) for hydration in a 5% CO<sub>2</sub> incubator at 37°C for 2 hours. The glioma cells were harvested and counted 24 h after transfection and inoculated in a chamber at a density of  $5 \times 10^4$  cells/well. The medium in the chamber was DMEM + 0.1% BSA, and the medium in the lower chamber was DMEM + 15% FBS, observed its effect on the migration ability of glioma cells, then removed the chamber after 24 h, fix the cells on the chamber membrane with 4% paraformaldehyde, and then stained with 0.1% crystal violet while the cells which did not pass through the membrane were wiped with a cotton swab, and the cells were photographed under high magnification (200 $\times$ ) and observed ten random fields of view, and the results were analyzed. For invasion assays, the chambers were coated with 90  $\mu$ l 0.8 mg/ml Matrigel and the subsequent steps were similar to the migraton assays.

### Tumor Xenograft in Nude Mice

U87 cells transfected with siRNA negative control or ANXA1 interference sequence for 48 h, harvested and

adjusted to a cell concentration of  $1 \times 10^7$  cells/ml,  $2 \times 10^6$  cells containing siRNA negative control or ANXA1 interference sequence in 200  $\mu$ l of PBS were then injected subcutaneously into on the both sides of mice. The tumor volume was monitored from day 3, tumor size was measured every 3 days, and tumor volume was calculated according to the formula (Volume =  $0.5 \times$  tumor width<sup>2</sup>  $\times$  length), depicting tumor growth curve. Tumor tissues were taken for weighing on the 30th day.

### ELISA Method to Detect the Release Level of VEGF

Each group of U87 cells was cultured for 48 h after transfection, and the cell culture supernatant was collected. All reagents were equilibrated to room temperature. The procedure was performed according to the manufacturer's protocols, using an EnSpire Manager spectrophotometer plate reader (Turku, Singapore) at 450 nm. The absorbance (A) values of the samples of each group were measured, and the concentration of VEGF in the samples was calculated by a standard curve.

### Assay of Cytosolic Phospholipase A2 (cPLA2) Activity

The cPLA2 activity was assayed by using sonicated liposomes prepared and 1-stearoyl-2-[1-<sup>14</sup>C]-arachidonyl-*sn*-glycero-3-phosphocholine as the substrate as described previously (Kim et al., 2001).

### Nuclear Factor NF- $\kappa$ B p65 Transcription Factor Activity Assay

After transfection for 48 h, U87 nuclear extracts were prepared using the NE-PER Nuclear and Cytoplasmic Extraction Reagents (ThermoFisher Scientific; 78833). Nuclear factor (NF)  $\kappa$ B activity was detected using 9  $\mu$ g of nuclear extract and an NF- $\kappa$ B p65 Transcription Factor Assay Kit (ab133112, Abcam, Cambridge, MA, USA) in accordance with manufacturer's protocols. Absorbance was measured with EnSpire Manager spectrophotometer plate reader (Turku, Singapore) at 450 nm.

### Immunohistochemical Analysis and Immunofluorescent Staining

The expression of ANXA1 in glioma tissues and normal brain tissues was examined by immunohistochemistry using a rabbit polyclonal antibody against ANXA1 (1:100). Five-micrometer sections were cut from paraffin-embedded brain tissue blocks, deparaffinized and rehydrated, then blocked endogenous peroxidase. The sections were boiled in citrate buffer (pH6.0) for 20 min for antigen retrieval. Thereafter, the sections were incubated with primary anti-ANXA1 antibody at

4°C overnight. Then the sections were incubated with corresponding biotinylated secondary antibody (DAKO, Demark), developed with ABC reagent kits and counterstained with Mayer's hematoxylin. After the photographed, the two pathologists scored in a double-blind case. The staining intensity was scored: 3 points for strong; 2 points for moderate; 1 point for weak; 0 points for no staining. The score was based on the percentage of ANXA1-positive cells: positive cells <5% was 0; 5% to 10% was 1; 10% to 50% was 2; 50% to 80% was 3; >80% was 4. The total score ranged from 0 to 12. The above two scores are multiplied by  $\geq 4$  to be positive, and  $< 4$  to be negative. For immunofluorescent staining, the glioma cells were then incubated with specific primary antibodies [anti-ANXA1 (1:200, sc-12740)] overnight at 4°C. Subsequently, the samples were rinsed three times with PBS containing 0.25% Tween-20 and incubated with secondary antibodies for 60 min at room temperature, and the nuclei were counterstained with DAPI. The cells were examined and counted immediately under fluorescence microscopy (IX81, Olympus, Tokyo, Japan).

### Gelatin Zymography

To measure MMP-2 and MMP-9 activity in U87 cells, gelatin zymography was performed as described previously (Morioka et al., 2019). Briefly, after transfection for 48 h, the supernatants of glioma cells were collected, and the supernatants were then prepared samples with loading buffer (125 mM Tris-HCl, pH 6.8, 1% glycerol, 2% SDS, 0.01% bromophenol blue) without heating or reduction, and separated by electrophoresis on an 8% SDS-polyacrylamide gel containing 0.1% w/v gelatin. After separation, the gels were gently washed thrice with distilled water containing 2.0% Triton X-100 for 1 hour to remove SDS, and further incubated with the substrate buffer (50 mM Tris-HCl containing 10 mM CaCl<sub>2</sub> and 0.02% NaN<sub>3</sub>, pH 7.6) at 37°C overnight, followed by staining with Coomassie Brilliant Blue R-250 for 1 h, and decolorized in 20% methanol and 10% acetic acid until clear bands appeared, and the density was measured with Image J software (Fuji Film, Tokyo, Japan).

### Statistical Analysis

Swth GraphPad Prism 5 program was used for statistical analysis. All data were expressed as mean  $\pm$  standard deviation. One-way analysis of variance and Student's *t*-test were performed to analyze these data, multiple comparison between the groups were analyzed by Bonferroni's multiple comparison method. The test level was  $\alpha = 0.05$ .

## Results

### *ANXA1 Is Upregulated in Glioma Cell Lines and Glioma Tissues*

The expression level of ANXA1 in glioma was measured in human astrocytes (NHA and HEB) and four glioma cell lines (U87, U251, U118, A172) by Western blot. ANXA1 was prominently up-regulated in glioma cell lines compared with human astrocytes (Figure 1A and B). Furthermore, we analyzed ANXA1 expression levels in glioma patients at different tumor stages and normal brain using IHC. The results showed that ANXA1 expression levels in grade III astrocytomas and GBM were evidently higher than those in the grade II astrocytomas, and ANXA1 expression levels in grade IV gliomas were significantly higher than those in grade III gliomas (Figure 1C and D). Similarly, we found ANXA1 protein expression was also significantly up-regulated in GBM compared with the normal brain tissue by Western blot (Figure 1E). Collectively, these results indicated that ANXA1 played an important role in the occurrence and development of glioma.

### *Knock Down of ANXA1 Inhibits Glioma Cell Proliferation, Migration and Invasion*

ANXA1 expression levels in U87, U251, U118 and A172 glioma cell lines were significantly higher than those in the NHA and HEB normal human astrocyte cell lines, and U87 showed the highest level of ANXA1 (Figure 1B). Then we further explored the function of ANXA1 in gliomas by using siRNA interference technology to transfect siRNA-NC and siRNA-ANXA1 into U87 cells. After transfecting 3 siRNAs into U87 cells for 48 h, Real-time PCR and Western blot confirmed a significant decrease in the expression of ANXA1 in human U87 cells transfected with siRNA-ANXA1 compared to the siRNA-NC (Figure 2A to C). The second siRNA sequence was the most efficient, and thus the second one was used in the following experiments. Subsequently, transfected U87 cells were cultured for 4 days for cell viability determination. CCK8 assay demonstrated that after siRNA-ANXA1 transfection, cellular growth of U87 cells was significantly inhibited compared to that of siRNA-NC (Figure 2D). We further analyzed the role of ANXA1 on glioma cell migration and invasion. After siRNA-ANXA1 transfection of U87 cells, the number of migrated and invaded cells was significantly reduced compared to that of cells transfected with siRNA-NC and untreated cells (Figure 2H to J). Moreover, to determine if the effects of ANXA1 on proliferation, migration and invasion selectively occur in glioma cells, we also knocked-down ANXA1 in normal HEB human cells (Figure 2E and F),

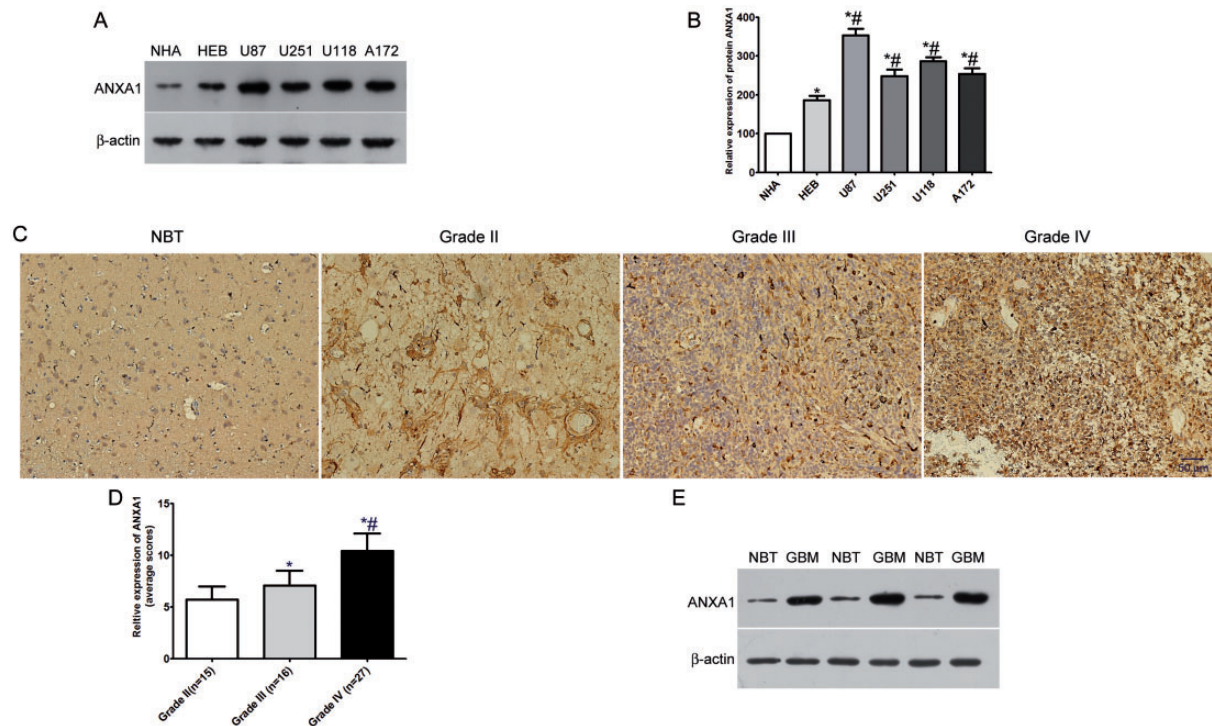


**Figure 1.** ANXA1 Expression Levels in Glioma Cells and Glioma Patients. A: Western blotting analysis of the expression levels of ANXA1 in human astrocytes (NHA and HEB) and glioma cell lines (U87, U251, U118 & A172). B: Quantification of the protein bands as shown in (A), \* $p < 0.05$  compared with NHA cells, # $p < 0.05$  compared with HEB cells. C: Representative immunohistochemistry images show that ANXA1 is more highly expressed in glioma tissues than in non-tumor brain tissues (NBT). Stronger stain intensity and higher stain density exist in glioblastoma tissues than those in non-tumor brain tissues. D: ANXA1 expression levels in glioma patients with different grades, \* $p < 0.05$  compared with Grade I group, # $p < 0.05$  compared with Grade II group. E: Western blot assays of ANXA1 expression in 3 non-tumor brain tissues (NBT) and 3 primary glioblastoma (Grade IV) tissues.

the results showed that after siRNA-ANXA1 transfection of HEB cells, the proliferation, migration and invasion of HEB cells were also significantly inhibited compared with siRNA-NC group (Figure 2G, K, L and M), and the data suggest that the inhibition effect was less than that observed in the U87 cells. These results demonstrated that down-expression of ANXA1 inhibited glioma cell proliferation, migration and invasion but also impaired proliferation and migration of normal HEB cells that had elevated ANXA1 expression compared to NHA.

### Knock Down of ANXA1 Arrested Glioma Cell Cycle and Induced Glioma Cell Apoptosis

Flow cytometry assay was employed to analyze cell cycle progression and apoptosis after siRNA-ANXA1 transfection in U87 cells. The results showed that an increase in the G2 phase and a decrease in the G1 phase of the cell cycle in ANXA1 down-regulated cells compared with siRNA-NC and untreated cells (Figure 3A and B). Furthermore, we analyzed the effects of ANXA1 on glioma cell apoptosis. The results showed that there

were significant apoptotic peaks in the siRNA-ANXA1 compared to those in cells transfected with siRNA-NC and untreated cells (Figure 3E and F). As done for proliferation, migration, and invasion, we also tested if the effects of ANXA1 on cell cycle distribution and apoptosis were selective glioma cells by knocking down ANXA1 in HEB astrocytes, the results showed that siRNA-ANXA1 transfection of HEB cells also significantly caused G2 phase arrest and promoted cellular apoptosis compared with siRNA-NC group (Figure 3C, D, G and H). These data demonstrated that down-regulation of ANXA1 can cause cell cycle arrest, consequently promoting cellular apoptosis. Moreover, to elucidate the association of ANXA1 levels with cell viability, we performed immunofluorescence staining at different time course after ANXA1 knockdown, the results revealed that ANXA1 began to decrease after transfection for 6 h, while apoptotic cells were fewer (Figure 3I, left panel), and showed significantly ANXA1 down-regulation and cell apoptosis at 48 h, there was an obvious negative correlation between ANXA1 levels and cell apoptosis (Figure 3I, right panel), specifically, the only survivors still had moderate-to-high ANXA1 levels in si-ANXA1

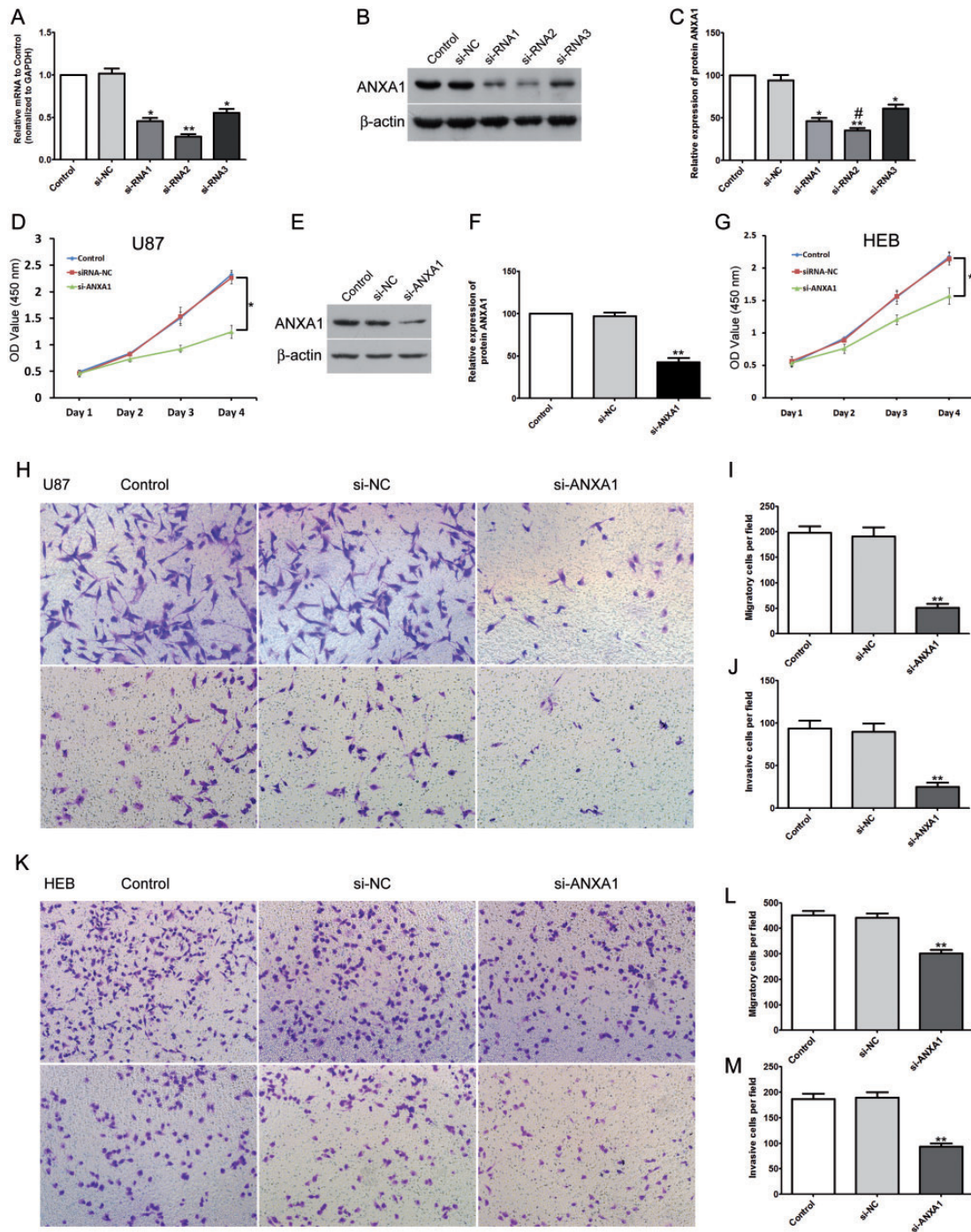


**Figure 2.** Down-Expression of ANXA1 Inhibited Glioma Cell and Normal Astrocytes Proliferation, Migration and Invasion. A: RT-qPCR results of the mRNA expression levels of ANXA1 in three groups transfected with ANXA1-siRNA in U87 cells. B: Western blot assay of ANXA1 levels in three groups transfected with ANXA1-siRNA in U87 cells. C: Quantification of the band intensity of ANXA1 in the Western blot in (B). \* $p < 0.05$ , \*\* $p < 0.01$  compared with si-NC group, # $p < 0.05$  compared with si-RNA1 group. D: After transfecting siRNA-ANXA1 into U87 cells, the cells proliferation activity was detected by CCK8 assay at the indicated time. E: Western blot assay of ANXA1 levels in HEB cells transfected with ANXA1-siRNA. F: Quantification of the band intensity of ANXA1 in the Western blot in E. \*\* $p < 0.01$  compared with si-NC group. G: After transfecting siRNA-ANXA1 into HEB cells, the cells proliferation activity was detected by CCK8 assay at the indicated time. H: Transwell assay exhibits the migration (upper panel) and invasion (lower panel) of U87 cells transfected with siRNA-ANXA1, siRNA-negative control (si-NC) group and blank control group. I and J: The quantitative statistics of the migration and invasion of U87 cells transfected with siRNA-ANXA1, si-NC group and control group. K: Transwell assay exhibits the migration (upper panel) and invasion (lower panel) of HEB cells transfected with siRNA-ANXA1, siRNA-negative control (si-NC) group and blank control group. L and M: The quantitative statistics of the migration and invasion of HEB cells transfected with siRNA-ANXA1, si-NC group and control group. All data are shown as mean  $\pm$  SD from at least three independent experiments, \* $p < 0.05$ , \*\* $p < 0.01$  compared with si-NC group.

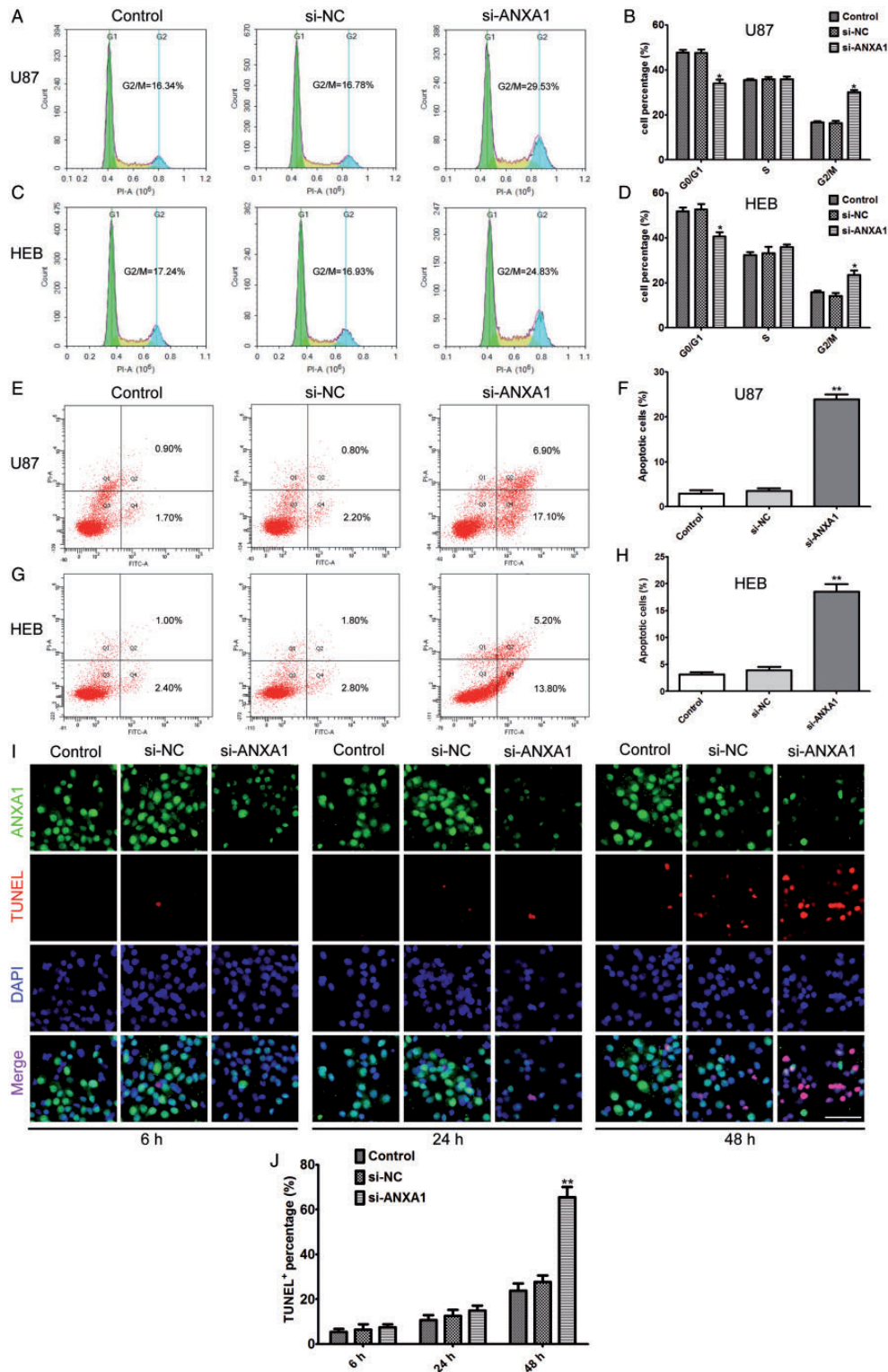


**Figure 3.** Knock-Down of ANXA1 Arrested Cell Cycle and Induced Cell Apoptosis. A and C: After siRNA-ANXA1 transfection of U87 and HEB cells, the cell cycle distribution was examined by Flow cytometry analysis. Decreasing ANXA1 expression resulted in a significant increase in the G2/M phase and a decrease in the G1 phase. B and D: Statistical analysis of the data shown in (A) and (C). E and G: After siRNA-ANXA1 transfection of U87 and HEB cells, the cell apoptosis rate was detected by Flow cytometry analysis. Decreasing ANXA1 expression resulted in a significant increase the proportion of apoptosis cells. F and H: Statistical analysis of the data shown in (E) and (G). I: Representative images of ANXA1 expression in control, si-NC and si-ANXA1 U87 cells after transfected for 6, 24 and 48 h, the cells were subjected to double staining for ANXA1 and TUNEL, and nuclei were counterstained with DAPI, Scale bar = 40  $\mu$ m. J: Quantitative analysis of the percentage of TUNEL positive staining cells at the indicated time points after transfected with si-NC and si-ANXA1 in U87 cells. In all graphs, the data are expressed as the mean  $\pm$  SD from three independent experiments. \* $p < 0.05$ , \*\* $p < 0.01$  compared with si-NC group.



transfection group, whereas the ANXA1 levels showed no significant changes in si-NC transfection group at different time courses compared with corresponding control group (Figure 3I and J), which corroborated that ANXA1 plays a pivotal role in apoptosis.

### Knock Down of ANXA1 Inhibits Tumor Size In Vivo

After establishing a causative relationship between the down-regulation of ANXA1 and glioma cell growth, we further confirmed whether decreasing ANXA1 might suppress tumor size in vivo. The effect of ANXA1 down-regulation on U87 tumor size in vivo was studied by subcutaneous injection of same amounts of U87/siRNA-ANXA1 or U87/siRNA-NC cells into either side of the same nude mouse. Four weeks later, the tumor formed by U87/siRNA-ANXA1 was significantly

smaller than those formed by U87/siRNA-NC cells (Figure 4A). The growth kinetic curve of U87/siRNA-ANXA1 tumors was compared to that of U87/siRNA-NC tumors (Figure 4B). Finally, the weight of tumors formed by U87/siRNA-ANXA1 cells was significantly decreased as compared to that formed by U87/siRNA-NC (Figure 4C). The down-regulation of ANXA1 in tumors formed by U87/siRNA-ANXA1 cells was further confirmed by Western blotting analysis (Figure 4D and E). These results demonstrated an inhibitory effect of ANXA1 on glioma cell growth *in vivo*.

### Inhibition of ANXA1 Induces G2/M Cell Cycle Arrest and by Inhibiting the PI3K/Akt Signaling Pathway

To understand the molecular mechanisms by which ANXA1 controlled glioma cell proliferation, migration

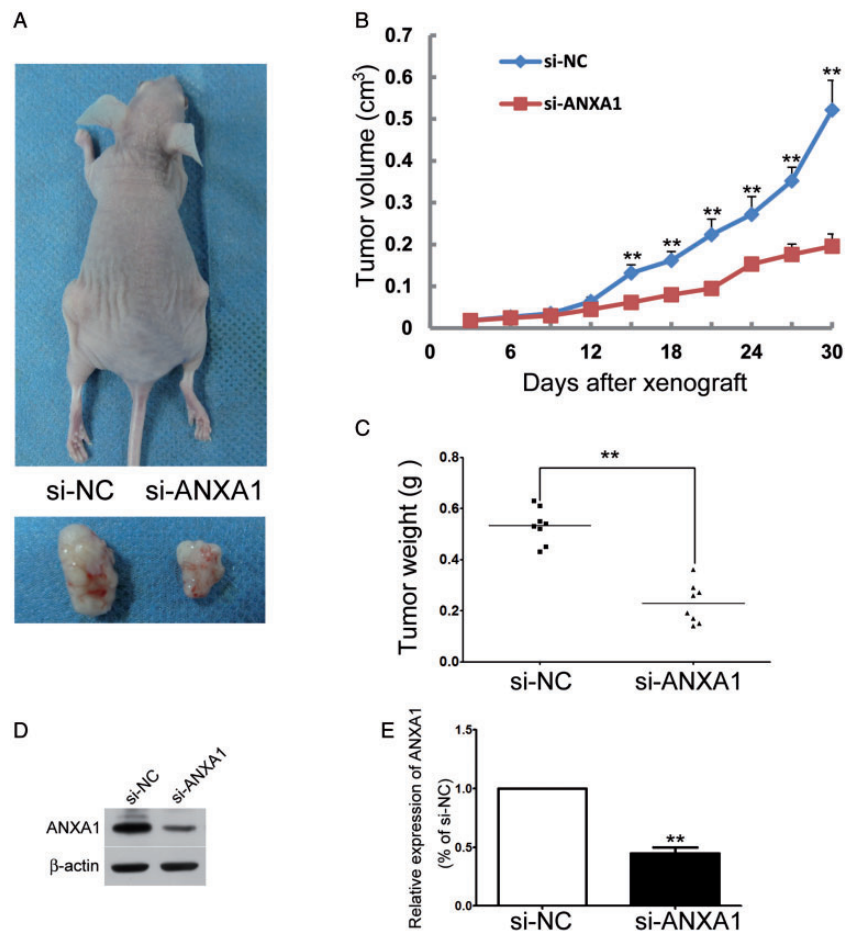


**Figure 4.** Knock Down of ANXA1 Inhibits Tumor Size In Vivo. A: Representative tumor-bearing nude mouse and the xenografted tumor derived from either U87/si-NC cells (left side) or U87/si-ANXA1 cells (right side). B: Statistic analysis demonstrated that the tumor volume derived from U87/si-ANXA1 cells increased more slowly than that of U87/si-NC cells after s.c. injection for 15 days, indicating that proliferation of U87/si-ANXA1 cells was suppressed by ANXA1 siRNA.  $**p < 0.01$  versus corresponding siRNA-NC controls, Mann-Whitney test,  $n = 8$ . C: Statistic analysis demonstrated that the tumor weight derived from U87/si-ANXA1 cells was significantly decreased as compared to that of U87/si-NC cells.  $**p < 0.01$ , Mann-Whitney test,  $n = 8$ . D: Western blot showed that ANXA1 was inhibited in tumors derived from U87/si-ANXA1 cells. E: The relative amounts of ANXA1 were quantified by a densitometric analysis (Image).

and invasion, we explored the effect of ANXA1 on expression levels of cell cycle-related proteins and several key signal pathways, which are closely related to the above mentioned biological function of glioma cells (M. Chen et al., 2019; Wei et al., 2019). Western blot analysis showed that ANXA1 had a prominent effect on cdc25C, cdc2 and cyclin B1 protein levels and PI3K/Akt signaling cascades but had no effect on cyclin D1, GSK-3 $\beta$  or  $\beta$ -catenin signaling in U87 cells (Figure 5A to D). In addition, whether ANXA1 regulates NF- $\kappa$ B and phospholipase A2 activity in glioma is still obscure, we also determined the expression and activity of NF- $\kappa$ B and cytosolic phospholipase A2 (cPLA2) in ANXA1 knock-down U87 cells, and NF- $\kappa$ B had no significant change between these groups, whereas decreasing ANXA1 expression significantly up-regulated cPLA2 expression and activity (Figure 5E to H). Therefore, down-regulation of ANXA1 expression suppressed expression

of cdc25C, cdc2, cyclin B1 and activation of the PI3K/Akt pathway, which may explain the impaired cell proliferation and invasion ability observed *in vitro* and *in vivo*.

### Effects of Activating or Blocking the PI3K/Akt Signaling Pathway on Cell Invasion and Migration in U87 Cells After siRNA-ANXA1 Transfection

To further reverse validate that down-regulated ANXA1 inhibits glioma proliferation, migration and invasion through the PI3K/Akt signaling pathway, IGF-1 and LY294002 were used to activate and inhibit the PI3K/Akt signaling pathway, respectively. The results showed that after transfection of siRNA-ANXA1 and addition of IGF-1, there were no significant differences in cell proliferation (Figure 6A), migration (Figure 6B) and invasion (Figure 6C) in U87 cells compared to cells

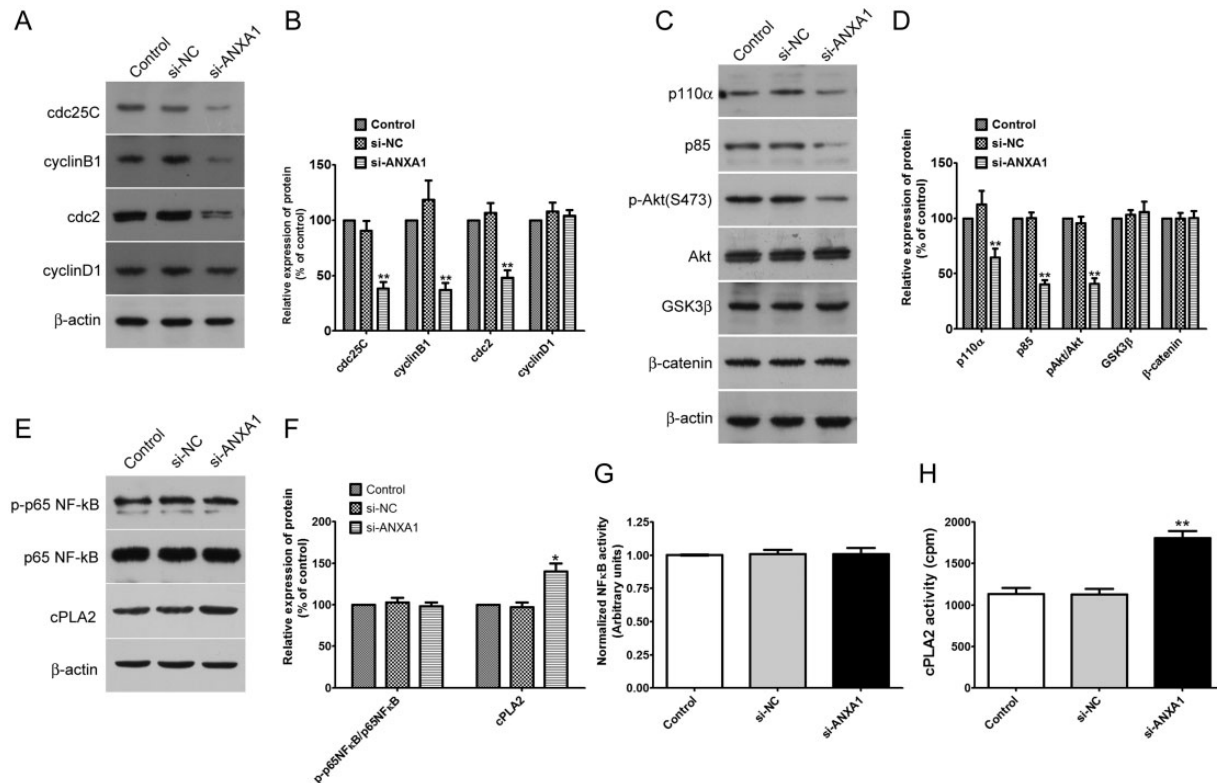


**Figure 5.** Knockdown ANXA1 Induces G2/M Cell Cycle Arrest in Glioma Cells via the PI3K/Akt Signaling Pathway. A: Inhibition of ANXA1 decreases the expression of cdc25C, cyclin B1 and cdc2, whereas cyclin D1 was not altered evidently. Western blot assay analysis was performed using anti-cdc25C, anti-cyclin B1, anti-cyclin D1, anti- $\beta$ -actin and anti-cdc2 antibodies. B: The relative amounts of cdc-25C, cyclin B1, cdc2 and Cyclin D1 were quantified by a densitometric analysis (ImageJ). C: Western blot analysis of PI3K subunit p110  $\alpha$  and p85, phosphorylation and total protein levels of Akt, GSK3  $\beta$  and  $\beta$ -catenin after si-ANXA1 or si-NC transfection for 48 h. D: Quantitative charts of phosphorylation and the total level of Akt, PI3K subunit p110  $\alpha$  and p85, GSK3  $\beta$  and  $\beta$ -catenin. E: Inhibition of ANXA1 has no effect on the expression of p-p65NF- $\kappa$ B and up-regulates the expression of cPLA2. Western blot assay analysis was performed using anti-p-p65NF- $\kappa$ B, anti-p65NF- $\kappa$ B, anti-cPLA2 and anti- $\beta$ -actin antibodies. F: The relative amounts of p-p65NF- $\kappa$ B and cPLA2 were quantified by a densitometric analysis (ImageJ). G: ELISA analysis of nuclear NF- $\kappa$ B activity. N = 9 per group. H: cPLA2 activity in control, si-NC and si-ANXA1 U87 cells. cPLA2 activity was determined as described in Methods. These results were expressed as the mean  $\pm$  SD from three independent experiments, \* $p$  < 0.05, \*\* $p$  < 0.01 compared with si-NC group.

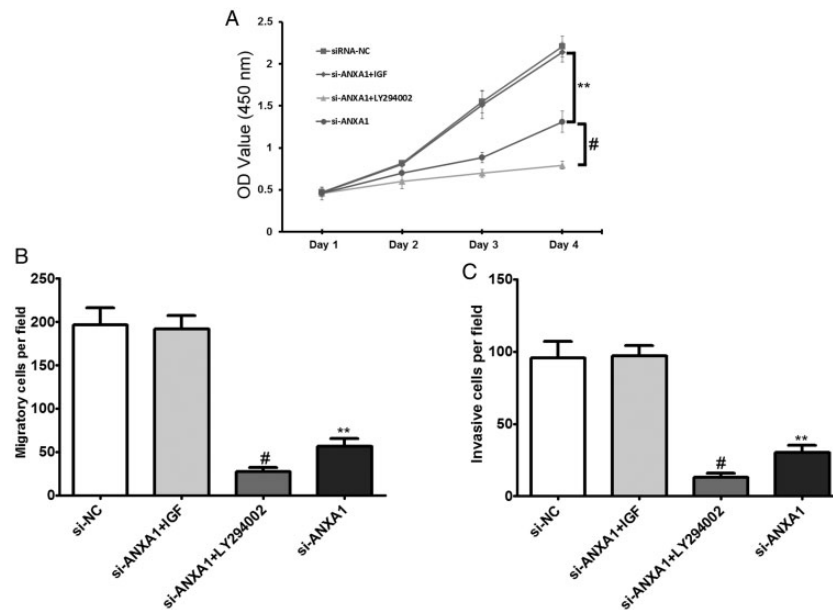


**Figure 6.** Effects of Activating or Blocking the PI3K/Akt Signaling Pathway on Cell Invasion and Migration in U87 Cells After siRNA-ANXA1 Transfection. A: After siRNA-ANXA1 transfection or together treated with IGF-I and LY294002 in U87 cells, the cells proliferation activity was detected by CCK8 assay. B: After siRNA-ANXA1 transfection or together treated with IGF-I and LY294002 in U87 cells, the cell migratory abilities were detected by Transwell assays. C: After siRNA-ANXA1 transfection or together treated with IGF-I and LY294002 in U87 cells, the cell invasive abilities were detected by transwell assays. All data are expressed as mean  $\pm$  SD from at least three independent experiments,  $**p < 0.01$  compared with si-NC group,  $\#p < 0.05$  compared with si-ANXA1 group.

transfected with siRNA-NC alone. After transfection of siRNA-ANXA1 and addition of LY294002, cell proliferation, migration and invasion in U87 cells were significantly lower than those in the siRNA-NC transfection only group and siRNA-ANXA1 transfection only group (Figure 6A to C). This suggests that down-regulation of ANXA1 inhibits activation of the PI3K/Akt signaling pathway to inhibit glioma cell proliferation, migration, and invasion.

### Inhibition of ANXA1 Down-Regulates MMP-2/-9 Expression

To better understand the molecular mechanisms involved in the process of migration and invasion after ANXA1 inhibition, we measured the expressions, activity and secretion of MMP-2, MMP-9 and VEGF in the glioma cells or the supernatant of cell culture medium after siRNA-ANXA1 transfection. Western blot analysis showed that decreasing ANXA1 expression significantly decreased MMP-2/-9 expressions (Figure 7A and B). Furthermore, gelatin zymography showed that decreasing ANXA1 expression tremendously decreased the activity of MMP-2/-9 released into the cultured medium (Figure 7D and E), whereas had no effect on VEGF expression or production compared to that of siRNA-NC and no treated cells (Figure 7A to C).

These data demonstrated that ANXA1 down-regulation inhibited glioma cell migration and invasion via down-regulating the expression and activity of MMP-2/-9. Thus, ANXA1//MMP-2/-9 axis plays a vital role on the migration and invasion of glioma cells.

## Discussion

Annexin-A1 has been demonstrated to be involved in various physiological and pathological processes. Accumulating evidence has suggested that Annexin-A1 plays an essential role in cell proliferation, phagocytosis, inflammation and apoptosis, as well as the development of tumors (Foo et al., 2019). However, whether ANXA1 is a oncogene or a tumor suppressor gene remains controversial, ANXA1 has been found to be up-regulated in gastric cancer, liver cancer, pancreatic cancer and esophageal adenocarcinoma; it has been revealed to be down-regulated or even absent in breast cancer, prostate cancer and B-cell lymphoma (Shao et al., 2019). These inconsistencies may be caused by different tumor microenvironments which induce different phenotypes of ANXA1. Moreover, recent studies have showed that ANXA1 is up-regulated in gliomas, which exerts its effect through formyl peptide receptor 2 (Tadei et al., 2018), but the exact mechanisms involved is still unclear.

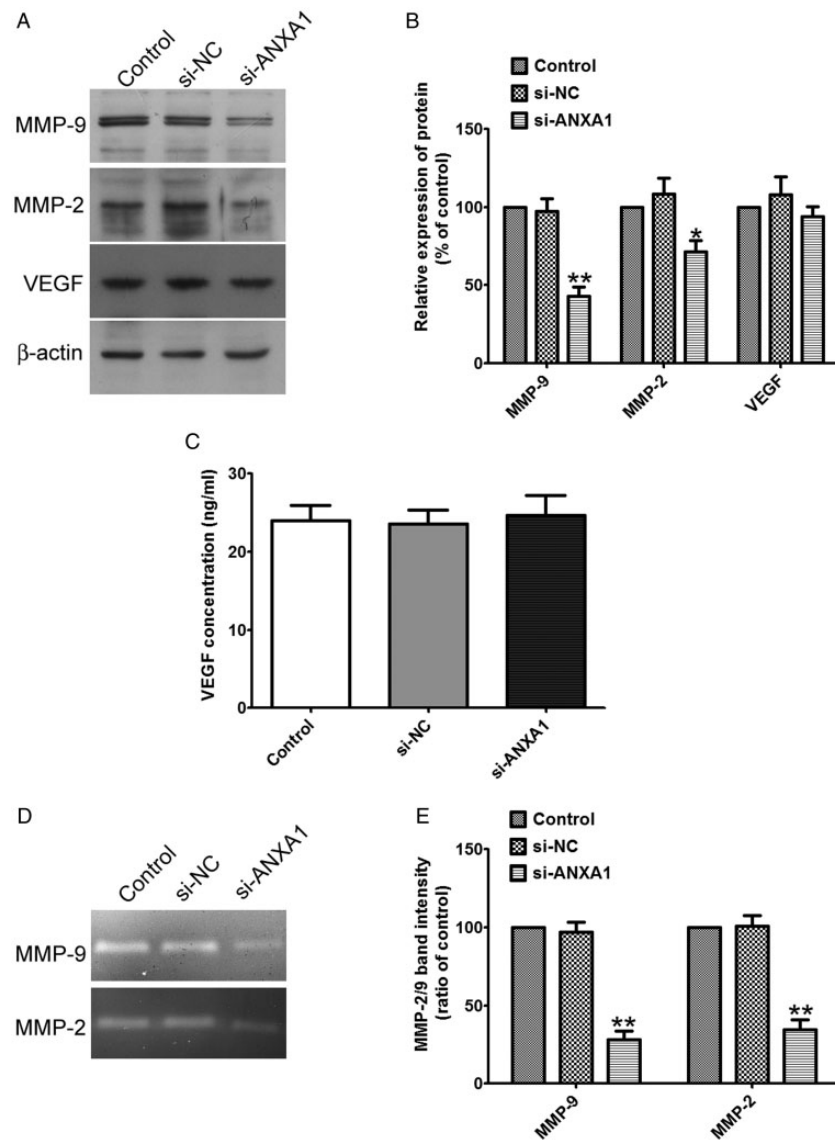


**Figure 7.** Knockdown ANXA1 Down-Regulates the Expression and Activity of MMP-2/9. **A:** Western blot analysis of total cell lysates isolated from glioma cells after si-ANXA1 or si-NC treatment by using the anti-MMP9, anti-MMP-2 and anti-VEGF antibodies. **B:** Quantitative charts of the protein levels of MMP2/9 and VEGF normalized to  $\beta$ -actin bands respectively. Data were expressed as the mean  $\pm$  SD from three independent experiments. **C:** U87 cells were planted ( $3 \times 10^5$  cells/well) in 24-well plates, after reaching 90% confluence, the cells were transfected with si-ANXA1 or si-NC, the secreted VEGF protein was then measured in the supernatants by ELISA. Data are presented as ng/mL VEGF (mean  $\pm$  SD,  $n = 5$  wells per condition). **D:** U87 cells were planted ( $3 \times 10^5$  cells/well) in 24-well plates, after reaching 90% confluence, the cells were transfected with si-ANXA1 or si-NC, the activity of MMP-2 and MMP-9 was then measured by gelatin zymography. **E:** Quantitative intensities of MMP-2/9 bands of relative histograms are shown. Data are expressed as the mean  $\pm$  SD from four independent experiments, \* $p < 0.05$  compared with si-NC group.

Tadei *et al.* found that ANXA1 is significantly higher in gliomas and its correlation with matrix metalloproteinase in gliomas tissues (Tadei *et al.*, 2018). This suggests that ANXA1 plays an important role in tumor development. In this study, we measured ANXA1 expression levels in glioma tissues and glioma cells. These data demonstrated that the expression levels of ANXA1 was more higher in glioma tissues and cells than that in normal brains and human astrocytes, and we further found

that ANXA1 expression levels in patients were intensely related with the degree of malignancy of primary human gliomas. This suggests that ANXA1 is closely related to the development and progression of glioma. Cellular experiments were performed to validate the effects of ANXA1 on gliomas. Both mRNA and protein data showed that ANXA1 expression levels in siRNA-ANXA1 transfection U87 or HEB cells were significantly inhibited. The decreased expression of ANXA1 led to a

significant decrease of the proliferation, migration and invasion capabilities of U87 and HEB cells. Additionally, decreasing ANXA1 expression significantly decreased the proportion of G<sub>0</sub>/G<sub>1</sub> phase cells and increased the proportion of G<sub>2</sub>/M phase cells, simultaneously inducing cellular apoptosis. Thus, ANXA1 down-regulation can induce cell cycle arrest at the G<sub>2</sub>/M phase and promote cellular apoptosis. In previous tumor studies, ANXA1 was found to be significantly elevated and able to promote tumor progression. Also, ANXA1 inhibition can significantly suppress tumor growth and induce apoptosis (Pessolano et al., 2018). This suggests that ANXA1 plays a key regulatory role as an oncogene in the occurrence and progression of tumors. In the subcutaneous tumor model, we found that knockdown ANXA1 significantly inhibited tumor growth rate and tumor weight, which consolidated our in vitro experimental results, however, the subcutaneous transplantation microenvironment couldn't represent for brain tumor microenvironment, and further studies remain to be continued.

Uncontrolled cellular proliferation is the most basic biological feature of cancer cells, and the disorder of cell cycle regulation is the root cause of uncontrolled proliferation (Malumbres and Barbacid, 2009). Therefore, the regulation of cell cycle has become one of the important ways of tumor treatment, just like the induction of apoptosis or necrosis. Cyclin is the main regulatory protein of eukaryotic cell cycle process. It regulates cell cycle by combining with cyclin dependent kinases (CDKs) to form cyclin CDKs complex. When tumor cells are treated with drugs or radiation, they usually have G<sub>1</sub>/S or G<sub>2</sub>/M phase arrest to repair damaged DNA. Cdc2 (cyclin-dependent kinase1)/cyclin B1 as an important switch of G<sub>2</sub>/M phase checkpoint (De Souza et al., 2000; Butz et al., 2017). It interacts with cdc25c in cell cycle and initiates the process of cell mitosis. In G<sub>2</sub>/M transmission, the protein complex named M phase-promoting factor that compose of cdc2 (catalytic) and cyclin B1 (regulatory) subunits plays a pivotal role. The dephosphorylation of cdc2 leads to enhanced complex activity by protein phosphatase cdc25, which is composed of cdc25A, cdc25B, cdc25C in human cells. However, cdc25A mainly activates CDK2, a key part of S phase regulators, to overcome the G<sub>1</sub>/S and intra-S checkpoints, while cdc25B regulates the complexes containing cyclin A and cyclin B1 in the cytoplasm to allow mitotic entry and cdc25C is responsible for dephosphorylating the cyclin B1/cdc2 complex to overcome the G<sub>2</sub>/M checkpoint and to entry into mitosis. In the current study, we demonstrated that decreasing ANXA1 expression induced G<sub>2</sub>/M cell cycle arrest in U87 and HEB cells, the protein levels of cdc25C, cyclin B1 and cdc2 were down regulated, subsequently leading to inhibition of the activity of cdc2/cyclin B1 complex, thus G<sub>2</sub> phase

arrest occurred, whereas Alldridge *et al.* found that ANXA1 could suppress cell proliferation by depleting cyclin D1 expression (Alldridge and Bryant, 2003). These inconsistencies indicated that ANXA1 expression is highly tissue specific in different tumors.

To confirm whether the effects of ANXA1 on proliferation, migration and invasion specifically occur in glioma cells, we also observed its effects in normal HEB human cells. Similarly, knockdown ANXA1 also reduced the cells ability for proliferation, migration and invasion while promoting cell apoptosis of normal human gliocyte HEB cells. This raises the question of whether U251 and/or A172 that show only a slight elevation of ANXA1 compared to the non-tumor line HEB cells, would have similar tumor growth or whether such cells would be more like HEB cells. In addition it remains unclear whether over-expressing ANXA1 in HEB cells to a level close to the expression levels in U87, would render these cells more proliferative and perhaps invasive. However, glioma tissues and cells show higher expression of ANXA1 compared with normal brain tissues and normal human astrocytes. Moreover, a previous study have synthesized a 7-mer peptide conjugated to anticancer drug SN-38, which targeting ANXA1 expressed on the surface of tumor vasculature with no apparent side effects (Hatakeyama et al., 2011), thus we still have reason to believe that there is still a great hope in the treatment of glioma by targeting ANXA1.

The PI3K/Akt signaling pathway regulates cellular and physiological processes, such as cell proliferation, differentiation, cell cycle, apoptosis and motility. Additionally, previous studies have demonstrated PI3K/Akt signaling has a crucial role in maintaining the biological features in various cancer cells (Faes and Dormond, 2015; Alzahrani, 2019). ANXA1 analysis in different types of gliomas showed that there was exclusive overexpression in astrocytomas associated with PI3K/Akt pathway (Ruano et al., 2008). Moreover, ANXA1 overexpression promoted cancer progression association with PI3K/Akt in nasopharyngeal carcinoma cells (Zhu et al., 2018) and colorectal cancer (Hagihara et al., 2019), we previously asked whether ANXA1 overexpression is connected to PI3K/Akt pathway in glioma, and our results confirmed this hypothesis. To further validate that the role of ANXA1 in regulating glioma growth and the involvement of PI3K/Akt signaling pathway, IGF-1 was employed to activate the PI3K/Akt signaling pathway and LY294002 was applied to inhibit the PI3K/Akt signaling pathway (G. Chen et al., 2017). The results showed that after transfection of siRNA-ANXA and addition of IGF-1, there were no distinct differences in cell proliferation, invasion and migration in U87 cells compared to the cells that transfected with siRNA-NC. After transfection of siRNA-ANXA1 combined with LY294002, resulted in a significantly synergistic

inhibitory effect on cell proliferation, migration and invasion in U87 cells compared to the siRNA-NC transfection only group and siRNA-ANXA1 transfection only group. Thus, sustained activation of the PI3K/Akt signaling pathway can reverse the inhibitory effects of down-regulated ANXA1 on glioma cell proliferation, migration and invasion. Moreover, using LY294002 to inhibit PI3K/Akt signaling pathway can promote the inhibitory effects of decreasing ANXA1 expression on glioma cell proliferation, migration and invasion.

Matrix metalloproteins (MMPs) are involved in degrading the extracellular matrix in various pathophysiological processes, promoting tumor metastasis (Conlon and Murray, 2019). It has been demonstrated that MMP2, an important member of MMP family, can be targeted by Akt to promote glioblastoma metastasis (M. Chen et al., 2019). It has been shown that inhibition of PI3K and Akt led to suppression of MMP-2/-9 activity and protein levels in cancer cells (G. Chen et al., 2017). Moreover, Yi *et al.* have demonstrated that the expression of ANXA1 is independent of VEGF (Yi and Schnitzer, 2009), and our data corroborate with the previous findings. Nevertheless, whether ANXA1 could regulate of MMP-2/-9 expression or activity in glioblastoma has not been fully elucidated. Although the underlying mechanisms and the correlation of ANXA1, Akt activation, and MMP-2/-9 expression in glioma remain inexplicit, our study demonstrated the fact that ANXA1 is associated with activation of the PI3K/Akt signaling pathway, which contributes to MMP-2/-9 expression and activity, resulting in oncogenic microenvironment formation, which promotes migration and invasion of glioma.

In conclusion, our study demonstrated that ANXA1 plays an oncogenic role in glioma by facilitating cell mobility. ANXA1 is a novel regulator of proliferation, migration and invasion by activating the PI3K/Akt signaling pathway in glioma cells. This study contributes to the clarification of the oncogenic function of ANXA1 in glioma and indicates that targeting ANXA1 could be a potential therapeutic strategy for suppressing glioma proliferation and invasion. However, the data shown here suggest that down-regulation of ANXA1 could also result in cell death of normal cells, which would clearly limit its therapeutic value. Intriguingly, our group recently synthesized a cell-penetrating peptide derived by conjugating the trans-activator of transcription (Tat) domain to the ANXA1 nuclear translocation signal (NTS), and the Tat-NTS improved the survival of hippocampal neurons subjected to oxygen-glucose deprivation and reperfusion *in vitro*, while had little impact on neuronal apoptosis or cognitive function in sham-treated nonischemic animals (Li et al., 2019). Whether Tat-NTS has anti-tumor effect without apparent side effects on normal cells via inhibiting ANXA1 nuclear translocation remains to

be further studied, but this approach could provide a useful alternative approach for targeting ANXA1 in gliomas.

### Declaration of Conflicting Interests

The author(s) declared no potential conflicts of interest with respect to the research, authorship, and/or publication of this article.

### Funding

The author(s) disclosed receipt of the following financial support for the research, authorship, and/or publication of this article: This work was supported by a research grant provided by Excellent Youth Foundation of Health and Family Planning Commission of Wuhan Municipality (WX17Q10). All experiments were conducted in compliance with ARRIVE and Huazhong University of Science and Technology guidelines.

### ORCID iD

Zhenzhao Luo  <https://orcid.org/0000-0002-9463-9184>

### References

- Akhavan, D., Cloughesy, T. F., & Mischel, P. S. (2010). mTOR signaling in glioblastoma: Lessons learned from bench to bedside. *Neuro Oncol*, *12*(8), 882–889.
- Alldrige, L. C., & Bryant, C. E. (2003). Annexin 1 regulates cell proliferation by disruption of cell morphology and inhibition of cyclin D1 expression through sustained activation of the ERK1/2 MAPK signal. *Exp Cell Res*, *290*(1), 93–107.
- Alzahrani, A. S. (2019). PI3K/Akt/mTOR inhibitors in cancer: At the bench and bedside. *Semin Cancer Biol*, *59*, 125–132.
- Bai, X. F., Ni, X. G., Zhao, P., Liu, S. M., Wang, H. X., Guo, B., Zhou, L. P., Liu, F., Zhang, J. S., Wang, K., Xie, Y. Q., Shao, Y. F., & Zhao, X. H. (2004). Overexpression of annexin 1 in pancreatic cancer and its clinical significance. *World J Gastroenterol*, *10*(10), 1466–1470.
- Bizzarro, V., Belvedere, R., Milone, M. R., Pucci, B., Lombardi, R., Bruzzese, F., Popolo, A., Parente, L., Budillon, A., & Petrella, A. (2015). Annexin A1 is involved in the acquisition and maintenance of a stem cell-like/aggressive phenotype in prostate cancer cells with acquired resistance to zoledronic acid. *Oncotarget*, *6*(28), 25076–25092.
- Boudhraa, Z., Merle, C., Mazzocut, D., Chezal, J. M., Chambon, C., Miot-Noirault, E., Theisen, M., Bouchon, B., & Degoul, F. (2014). Characterization of pro-invasive mechanisms and N-terminal cleavage of ANXA1 in melanoma. *Arch Dermatol Res*, *306*(10), 903–914.
- Butz, H., Németh, K., Czenke, D., Likó, I., Czirják, S., Zivkovic, V., Baghy, K., Korbonits, M., Kovalszky, I., Igaz, P., Rác, K., & Patócs, A. (2017). Systematic investigation of expression of G2/M transition genes reveals CDC25 alteration in nonfunctioning pituitary adenomas. *Pathol Oncol Res*, *23*(3), 633–641.
- Chai, C., Song, L. J., Han, S. Y., Li, X. Q., & Li, M. (2018). MicroRNA-21 promotes glioma cell proliferation and inhibits senescence and apoptosis by targeting SPRY1 via the

- PTEN/PI3K/AKT signaling pathway. *CNS Neurosci Ther*, 24(5), 369–380.
- Chen, G., Yue, Y., Qin, J., Xiao, X., Ren, Q., & Xiao, B. (2017). Plumbagin suppresses the migration and invasion of glioma cells via downregulation of MMP-2/9 expression and inactivation of PI3K/Akt signaling pathway in vitro. *J Pharmacol Sci*, 134(1), 59–67.
- Chen, M., Yin, X., Lu, C., Chen, X., Ba, H., Cai, J., & Sun, J. (2019). Mahanine induces apoptosis, cell cycle arrest, inhibition of cell migration, invasion and PI3K/AKT/mTOR signalling pathway in glioma cells and inhibits tumor growth in vivo. *Chem Biol Interact*, 299, 1–7.
- Cheng, S. X., Tu, Y., & Zhang, S. (2013). FoxM1 promotes glioma cells progression by up-regulating Anxa1 expression. *PLoS One*, 8(8), e72376.
- Conlon, G. A., & Murray, G. I. (2019). Recent advances in understanding the roles of matrix metalloproteinases in tumour invasion and metastasis. *J Pathol*, 247(5), 629–640.
- Danielsen, S. A., Eide, P. W., Nesbakken, A., Guren, T., Leithe, E., & Lothe, R. A. (2015). Portrait of the PI3K/AKT pathway in colorectal cancer. *Biochim Biophys Acta*, 1855(1), 104–121.
- De Souza, C. P., Ellem, K. A., & Gabrielli, B. G. (2000). Centrosomal and cytoplasmic Cdc2/cyclin B1 activation precedes nuclear mitotic events. *Exp Cell Res*, 257(1), 11–21.
- Faes, S., & Dormond, O. (2015). PI3K and AKT: Unfaithful partners in cancer. *Int J Mol Sci*, 16(9), 21138–21152.
- Fatehi, M., Hunt, C., Ma, R., & Toyota, B. D. (2018). Persistent disparities in survival for patients with glioblastoma. *World Neurosurg*, 120, e511–e516.
- Foo, S. L., Yap, G., Cui, J., & Lim, L. H. K. (2019). Annexin-A1—A blessing or a curse in cancer? *Trends Mol Med*, 25(4), 315–327.
- Garcia Pedrero, J. M., Fernandez, M. P., Morgan, R. O., Herrero Zapatero, A., Gonzalez, M. V., Suarez Nieto, C., & Rodrigo, J. P. (2004). Annexin A1 down-regulation in head and neck cancer is associated with epithelial differentiation status. *Am J Pathol*, 164(1), 73–79.
- Gastardelo, T. S., Cunha, B. R., Raposo, L. S., Maniglia, J. V., Cury, P. M., Lisoni, F. C., Tajara, E. H., & Olinari, S. M. (2014). Inflammation and cancer: role of annexin A1 and FPR2/ALX in proliferation and metastasis in human laryngeal squamous cell carcinoma. *PLoS One*, 9(12), e111317.
- Górska, J., Raźny, U., Polus, A., Stancel-Moźwiłło, J., Chojnacka, M., Gruca, A., Zdzienicka, A., Dembińska-Kieć, A., Kieć-Wilk, B., Solnica, B., & Malczewska-Malec, M. (2018). Pro-inflammatory gene expression profile in obese adults with high plasma GIP levels. *Int J Obes (Lond)*, 42(4), 826–834.
- Guerrero-Zotano, A., Mayer, I. A., & Arteaga, C. L. (2016). PI3K/AKT/mTOR: role in breast cancer progression, drug resistance, and treatment. *Cancer Metastasis Rev*, 35(4), 515–524.
- Hagihara, T., Kondo, J., Endo, H., Ohue, M., Sakai, Y., & Inoue, M. (2019). Hydrodynamic stress stimulates growth of cell clusters via the ANXA1/PI3K/AKT axis in colorectal cancer. *Sci Rep*, 9(1), 20027.
- Hatakeyama, S., Sugihara, K., Shibata, T. K., Nakayama, J., Akama, T. O., Tamura, N., Wong, S. M., Bobkov, A. A., Takano, Y., Ohyama, C., Fukuda, M., & Fukuda, M. N. (2011). Targeted drug delivery to tumor vasculature by a carbohydrate mimetic peptide. *Proc Natl Acad Sci U S A*, 108(49), 19587–19592.
- Kan, T., & Meltzer, S. J. (2009). MicroRNAs in Barrett's esophagus and esophageal adenocarcinoma. *Curr Opin Pharmacol*, 9(6), 727–732.
- Kim, S. W., Rhee, H. J., Ko, J., Kim, Y. J., Kim, H. G., Yang, J. M., Choi, E. C., & Na, D. S. (2001). Inhibition of cytosolic phospholipase A2 by annexin I. Specific interaction model and mapping of the interaction site. *J Biol Chem*, 276(19), 15712–15719.
- Laplante, M., & Sabatini, D. M. (2009). mTOR signaling at a glance. *J Cell Sci*, 122(Pt 20), 3589–3594.
- Lei, X., Chang, L., Ye, W., Jiang, C., & Zhang, Z. (2015). Raf kinase inhibitor protein (RKIP) inhibits the cell migration and invasion in human glioma cell lines in vitro. *Int J Clin Exp Pathol*, 8(11), 14214–14220.
- Li, X., Zheng, L., Xia, Q., Liu, L., Mao, M., Zhou, H., Zhao, Y., & Shi, J. (2019). A novel cell-penetrating peptide protects against neuron apoptosis after cerebral ischemia by inhibiting the nuclear translocation of annexin A1. *Cell Death Differ*, 26(2), 260–275.
- Lim, L. H., & Pervaiz, S. (2007). Annexin 1: The new face of an old molecule. *FASEB J*, 21(4), 968–975.
- Liu, Y. F., Zhang, P. F., Li, M. Y., Li, Q. Q., & Chen, Z. C. (2011). Identification of annexin A1 as a proinvasive and prognostic factor for lung adenocarcinoma. *Clin Exp Metastasis*, 28(5), 413–425.
- Malumbres, M., & Barbacid, M. (2009). Cell cycle, CDKs and cancer: A changing paradigm. *Nat Rev Cancer*, 9(3), 153–166.
- Masaki, T., Tokuda, M., Ohnishi, M., Watanabe, S., Fujimura, T., Miyamoto, K., Itano, T., Matsui, H., Arima, K., Shirai, M., Maeba, T., Sogawa, K., Konishi, R., Taniguchi, K., Hatanaka, Y., Hatase, O., & Nishioka, M. (1996). Enhanced expression of the protein kinase substrate annexin in human hepatocellular carcinoma. *Hepatology*, 24(1), 72–81.
- Morioka, N., Kodama, K., Tomori, M., Yoshikawa, K., Saeki, M., Nakamura, Y., Zhang, F. F., Hisaoka-Nakashima, K., & Nakata, Y. (2019). Stimulation of nuclear receptor REV-ERBs suppresses production of pronociceptive molecules in cultured spinal astrocytes and ameliorates mechanical hypersensitivity of inflammatory and neuropathic pain of mice. *Brain Behav Immun*, 78, 116–130.
- Nishikawa, R. (2010). Standard therapy for glioblastoma—A review of where we are. *Neurol Med Chir (Tokyo)*, 50(9), 713–719.
- Pagliara, V., Adornetto, A., Mammì, M., Masullo, M., Sarnataro, D., Pietropaolo, C., & Arcone, R. (2014). Protease nexin-1 affects the migration and invasion of C6 glioma cells through the regulation of urokinase plasminogen activator and matrix metalloproteinase-9/2. *Biochim Biophys Acta*, 1843(11), 2631–2644.
- Patton, K. T., Chen, H. M., Joseph, L., & Yang, X. J. (2005). Decreased annexin I expression in prostatic adenocarcinoma and in high-grade prostatic intraepithelial neoplasia. *Histopathology*, 47(6), 597–601.

- Pessolano, E., Belvedere, R., Bizzarro, V., Franco, P., Marco, I., Porta, A., Tosco, A., Parente, L., Perretti, M., & Petrella, A. (2018). Annexin A1 may induce pancreatic cancer progression as a key player of extracellular vesicles effects as evidenced in the in vitro MIA PaCa-2 model system. *Int J Mol Sci*, *19*(12), 3878.
- Petrella, A., Festa, M., Ercolino, S. F., Zerilli, M., Stassi, G., Solito, E., & Parente, L. (2006). Annexin-1 downregulation in thyroid cancer correlates to the degree of tumor differentiation. *Cancer Biol Ther*, *5*(6), 643–647.
- Pin, A. L., Houle, F., Fournier, P., Guillonnet, M., Paquet É, R., Simard, M. J., Royal, I., & Huot, J. (2012). annexin-1-mediated endothelial cell migration and angiogenesis are regulated by vascular endothelial growth factor (VEGF)-induced inhibition of miR-196a expression. *J Biol Chem*, *287*(36), 30541–30551.
- Ruano, Y., Mollejo, M., Camacho, F. I., Rodríguez de Lope, A., Fiaño, C., Ribalta, T., Martínez, P., Hernández-Moneo, J. L., & Meléndez, B. (2008). Identification of survival-related genes of the phosphatidylinositol 3'-kinase signaling pathway in glioblastoma multiforme. *Cancer*, *112*(7), 1575–1584.
- Shao, G., Zhou, H., Zhang, Q., Jin, Y., & Fu, C. (2019). Advancements of annexin A1 in inflammation and tumorigenesis. *Onco Targets Ther*, *12*, 3245–3254.
- Sun, G., SiMa, G., Wu, C., Fan, Y., Tan, Y., Wang, Z., Cheng, G., & Li, J. (2018). Decreased MiR-17 in glioma cells increased cell viability and migration by increasing the expression of Cyclin D1, p-Akt and Akt. *PLoS One*, *13*(1), e0190515.
- Tadei, M. B., Mayorquim, M. V., de Souza, C. B., de Souza Costa, S., Possebon, L., Souza, H. R., Iyomasa-Pilon, M. M., Geromel, M. R., & Girol, A. P. (2018). Expression of the annexin A1 and its correlation with matrix metalloproteinases and the receptor for formylated peptide-2 in diffuse astrocytic tumors. *Ann Diagn Pathol*, *37*, 62–66.
- Wang, L. D., Yang, Y. H., Liu, Y., Song, H. T., Zhang, L. Y., & Li, P. L. (2008). Decreased expression of annexin A1 during the progression of cervical neoplasia. *J Int Med Res*, *36*(4), 665–672.
- Wang, X., Ding, J., & Meng, L. H. (2015). PI3K isoform-selective inhibitors: next-generation targeted cancer therapies. *Acta Pharmacol Sin*, *36*(10), 1170–1176.
- Wei, M., Cao, Y., Jia, D., Zhao, H., & Zhang, L. (2019). CREPT promotes glioma cell proliferation and invasion by activating Wnt/ $\beta$ -catenin pathway and is a novel target of microRNA-596. *Biochimie*, *162*, 116–124.
- Yang, Y., Liu, Y., Yao, X., Ping, Y., Jiang, T., Liu, Q., Xu, S., Huang, J., Mou, H., Gong, W., Chen, K., Bian, X., & Wang, J. M. (2011). Annexin 1 released by necrotic human glioblastoma cells stimulates tumor cell growth through the formyl peptide receptor 1. *Am J Pathol*, *179*(3), 1504–1512.
- Yi, M., & Schnitzer, J. E. (2009). Impaired tumor growth, metastasis, angiogenesis and wound healing in annexin A1-null mice. *Proc Natl Acad Sci U S A*, *106*(42), 17886–17891.
- Zhong, C., Li, X., Tao, B., Peng, L., Peng, T., Yang, X., Xia, X., & Chen, L. (2019). LIM and SH3 protein 1 induces glioma growth and invasion through PI3K/AKT signaling and epithelial-mesenchymal transition. *Biomed Pharmacother*, *116*, 109013.
- Zhu, J. F., Huang, W., Yi, H. M., Xiao, T., Li, J. Y., Feng, J., Yi, H., Lu, S. S., Li, X. H., Lu, R. H., He, Q. Y., & Xiao, Z. Q. (2018). Annexin A1-suppressed autophagy promotes nasopharyngeal carcinoma cell invasion and metastasis by PI3K/AKT signaling activation. *Cell Death Dis*, *9*(12), 1154.